International Journal of Control
Publication details, including instructions for authors and subscription information:
http://www.tandfonline.com/loi/tcon20

Motion planning for three-dimensional overhead cranes with high-speed load hoisting

H.-H. Lee
[a] Department of Mechanical Engineering, Tulane University, New Orleans, Louisiana 70118, USA

Available online: 20 Feb 2007

To cite this article: H.-H. Lee (2005): Motion planning for three-dimensional overhead cranes with high-speed load hoisting, International Journal of Control, 78:12, 875-886

To link to this article: http://dx.doi.org/10.1080/00207170500197571

International Journal of Control
Vol. 78, No. 12, 15 August 2005, 875–886

Motion planning for three-dimensional overhead cranes with high-speed load hoisting

H.-H. LEE*

Department of Mechanical Engineering, Tulane University, New Orleans, Louisiana 70118, USA

(*Received 7 February 2005; in final form 31 May 2005*)

This paper proposes a systematic anti-swing motion-planning method for three-dimensional overhead cranes, based on the load-swing dynamics of a two-dimensional overhead crane. First, a model-following anti-swing control law is designed based on the load-swing dynamics of a two-dimensional overhead crane, where the Lyapunov stability theorem is used as a mathematical tool. Then a new anti-swing motion-planning scheme is designed for a two-dimensional overhead crane based on the model-following anti-swing control law and typical crane operation in practice. Finally, the new anti-swing motion-planning scheme is extended for a three-dimensional overhead crane, based on the geometric relationship between a three-dimensional overhead crane and its two-dimensional counterpart. As a result, the proposed method avoids solving the load-swing dynamics of a three-dimensional overhead crane which is much more complicated than that of its two-dimensional counterpart. Furthermore, the proposed method can be applied to any existing overhead cranes without increasing their actuator torque capacity. The effectiveness of the proposed method is demonstrated by generating high-performance anti-swing trajectories with high-speed long-distance load hoisting.

1. Introduction

Over the past two decades, extensive research has been performed toward the anti-swing control of overhead cranes. In the anti-swing control, most of research efforts have been concerned with the anti-swing control of two-dimensional overhead cranes (d'Andrea-Novel and Boustany 1991, Yu *et al*. 1995, Yoshida 1998, Collado *et al*. 2000, Kiss *et al*. 2000, Singhose *et al*. 2000, Fang *et al*. 2003, Lee 2003), where the two-dimensional overhead cranes are those that allow one-dimensional trolley translation on a horizontal plane, with load hoisting, as shown in figure 1.

In some cases, however, the anti-swing control of three-dimensional overhead cranes is much more important and practical than that of two-dimensional overhead cranes, especially for factory and warehouse automation. The three-dimensional overhead cranes are those that allow two-dimensional trolley translation on a horizontal plane, with load hoisting, as shown in figure 3. One of the major problems in the anti-swing control of three-dimensional overhead cranes is that the dynamics of a three-dimensional overhead crane (Moustafa and Ebeid 1988, Lee 1998) are much more complicated than that of a two-dimensional overhead crane. As a result, the anti-swing control schemes for two-dimensional overhead cranes cannot be extended in most cases for three-dimensional overhead cranes, especially when considerable load hoisting is involved.

Crane operation in industry frequently requires high-speed load hoisting in the accelerating and decelerating zones of the trolley to avoid various obstacles in the workspace under the trolley. However, the existing anti-swing control schemes for three-dimensional overhead cranes have been designed under the constraints of no load hoisting (Moustafa and Ebeid 1988, Fang *et al*. 2001) or slow load hoisting (Lee 1998, Cho *et al*. 2002), which increases the travelling time of the trolley and hence reduces the work efficiency of the crane operation.

*Email: hhlee@tulane.edu

International Journal of Control
ISSN 0020–7179 print/ISSN 1366–5820 online © 2005 Taylor & Francis Group Ltd
http://www.tandf.co.uk/journals
DOI: 10.1080/00207170500197571

This implies that high-speed load hoisting should be allowed while cranes are in motion for a high-efficiency anti-swing control; therefore, high-performance anti-swing motion planning is required for such anti-swing control. However, little attention has been paid to systematic motion planning (Mita and Kanai 1979, Lee 2002, 2004).

Motion planning is a kinematic problem (Lee 2004), determining anti-swing trolley motion for given load-hoisting conditions without considering the required forces that cause such motion. Mita and Kanai (1979) solved a minimum-time trajectory-generation problem with fixed rope length, based on the load-swing dynamics linearized around the vertical stable equilibrium. Recently, Lee (2002, 2004) proposed motion-planning schemes based on the concept of minimum-time control and a regulating anti-swing control, which allows high-speed load hoisting. However, these existing anti-swing motion-planning schemes are effective only for two-dimensional overhead cranes. For three-dimensional overhead cranes, no motion-planning method allowing high-speed load hoisting is available yet, possibly due to the complexities of the dynamics of three-dimensional overhead cranes. Therefore, the objective of this study is to develop a practical anti-swing motion-planning method, allowing high-speed load hoisting, for three-dimensional overhead cranes.

This paper proposes a systematic motion-planning method for a high-performance anti-swing control of three-dimensional overhead cranes. First, a new model-following anti-swing control law is designed based on the load-swing dynamics of a two-dimensional overhead crane. The stability of the model-following anti-swing control law is proven using the Lyapunov stability theorem. Then a new anti-swing motion-planning scheme is developed for a two-dimensional overhead crane based on the proposed model-following anti-swing control law and typical anti-swing crane operation in practice. Finally, the anti-swing motion-planning scheme for a two-dimensional overhead crane is extended to that for a three-dimensional overhead crane by using their geometric relationship, instead of directly solving the complicated three-dimensional load-swing dynamics. This is well justified since the motion planning is not a dynamic problem, but a kinematic problem.

The proposed motion-planning scheme generates a typical anti-swing trajectory in industry for both two- and three-dimensional overhead cranes, with high-speed load hoisting. A favourable feature of the proposed method is that the anti-swing motion planning for three-dimensional overhead cranes is developed based on the load-swing dynamics of a two-dimensional overhead crane, which is much simpler than that of a three-dimensional overhead crane. Another important feature of the proposed method is that the proposed scheme is a motion-planning scheme, thus only generating desired anti-swing trajectories for given initial and goal positions. Therefore, with this proposed motion planning, an anti-swing trajectory control scheme should be used to actually control the motion of an overhead crane under parametric uncertainties and disturbances.

The proposed method has substantially improved the previous motion planning (Lee 2002, 2004) for a two-dimensional overhead crane. The previous method applies a minimum-time open-loop control and a regulating anti-swing control in series, in each of the accelerating and decelerating zones. Therefore, load swing is not controlled while the minimum-time control is applied, in which the trolley acceleration is assumed to be sufficient for a minimum-time control. As a result, the performance of trajectory generation deteriorates when the maximum available trolley acceleration is not large enough for a minimum-time control. Consequently, the actuator torque capacity of existing overhead cranes may have to be increased for most cases in order to adopt the previous method. However, the new method proposed in this study completely fixes this practical problem. The new method allows flexibility between the accelerating and decelerating intervals, and hence is flexible with the trolley acceleration. Therefore, the new method can be applied to any existing overhead cranes without increasing their actuator torque capacity.

As discussed above, the previous method (Lee 2002, 2004) applies a minimum-time open-loop control and a regulating anti-swing control in series, in each of the accelerating and decelerating zones. On the other hand, the new method applies a model-following anti-swing control throughout the entire motion-planning process. Therefore, the motion-planning processes for the previous and new methods are substantially different. The performance of the previous method is greatly affected by three parameters (the minimum-time control interval, the anti-swing control interval, and the maximum transient acceleration between these two controls) in each of the accelerating and decelerating zones. Therefore, fine tuning of the three parameters requires a great deal of experience and intuition; the previous method may cause a large jerk in the transition from the minimum-time control to the anti-swing control, depending on the value of the maximum transient acceleration. However, the new method completely solves all these problems since it eliminates those three parameters. The new method normally only brings about a little jerk and substantially simplifies the tuning process, thus resulting in easy implementation with guaranteed performance. A part of the preliminary result of the new method was presented at IMECE 2004 (Lee *et al*. 2004).

The remainder of this paper is organized as follows. In §2, the dynamic and kinematic models of a two-dimensional overhead crane are described. In §3, the anti-swing control problem is solved as a model-following control, based on the kinematic model. In §4, a systematic motion-planning scheme is proposed for a two-dimensional overhead crane, and in §5, the proposed motion-planning scheme is extended for a three-dimensional overhead crane. In §6, the proposed motion-planning scheme is evaluated. Finally, in §7, conclusions are drawn for this study.

2. Modelling of an overhead crane

2.1. *Dynamic model of an overhead crane*

Figure 1 shows the plane model of a two-dimensional overhead crane and its load, where r, θ, and l denote the trolley position, swing angle, and hoisting rope length, respectively.

In this study, the mass and stiffness of the hoisting rope are neglected and the load is considered as a point mass, which is valid with the usual multi-wire hoisting mechanisms in practice. Then the equations of motion of the crane system (Lee 1998) are obtained as

$$(m_r + m)\ddot{r} + ml\cos\theta\ddot{\theta} + m\sin\theta\ddot{l} + d_{vr}\dot{r} + 2m\cos\theta\dot{l}\dot{\theta} - ml\sin\theta\dot{\theta}^2 = f_r, \quad (1)$$

$$(m_l + m)\ddot{l} + m\sin\theta\ddot{r} + d_{vl}\dot{l} - ml\dot{\theta}^2 - mg\cos\theta = f_l, \quad (2)$$

$$ml^2\ddot{\theta} + ml\cos\theta\ddot{r} + 2ml\dot{l}\dot{\theta} + mgl\sin\theta = 0, \quad (3)$$

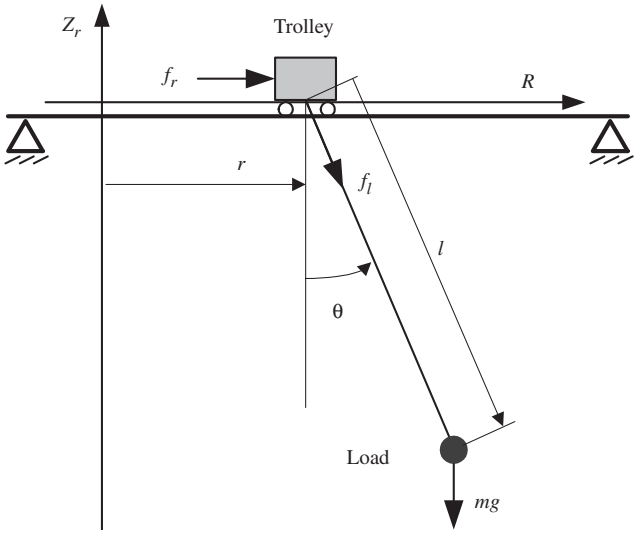

Figure 1. Plane model of a two-dimensional overhead crane.

where m is the load mass; m_r and m_l are the r (travelling) and l (hoisting down) components of the crane mass, respectively, which includes the equivalent masses of the rotating parts such as motors and their drive trains; d_{vr} and d_{vl} denote the viscous damping coefficients associated with the r and l motions, respectively; f_r and f_l are the driving forces for the r and l motions, respectively; g denotes the gravitational acceleration.

2.2. *Kinematic model for trajectory generation*

The load-swing dynamics (3) defines the kinematic relationship between the trolley acceleration as the input and the load swing as the output. For this reason, the load-swing dynamics can be considered as a kinematic equation for motion planning and can be rewritten as

$$l\ddot{\theta} + \cos\theta\ddot{r} + 2\dot{l}\dot{\theta} + g\sin\theta = 0. \quad (4)$$

All trackable anti-swing trajectories should satisfy the kinematic model (4). It should be noted that the kinematic model is independent of load mass m and hence contains no parametric uncertainties and disturbances for motion planning.

In this study, a new motion-planning scheme is designed based on the kinematic model (4). Therefore, the motion-planning scheme generates desired anti-swing reference trajectories that do not include any parametric uncertainties and disturbances. The effects of parametric uncertainties and disturbances should be suppressed by using an additional anti-swing trajectory control scheme, which should be designed based on the dynamic model (1)–(3).

3. Anti-swing control under high-speed load hoisting

In this section, the anti-swing control problem will be solved as a model-following control, based on the kinematic model (4), for a given high-speed load-hoisting motion (l, $\dot{l}$, and $\ddot{l}$).

Theorem 1: *Suppose that* r_r, $\dot{r}_r$, $\ddot{r}_r$, l, $\dot{l}$, *and* $\ddot{l}$ *are uniformly bounded and that* $l > 0$ *for all time* $t \geq 0$. *Then the following model-following anti-swing control law* (5) *guarantees that* $\theta, \dot{\theta}, \ddot{\theta}, \dot{r}, \ddot{r} \in L_\infty$ *if* $|\theta(0)| < \pi/2$, *and that* $\dot{\theta} \to 0$, $\theta \to 0$, *and* $\dot{r} \to \dot{r}_r$ *asymptotically as* $t \to \infty$ *if* $|\theta(0)| < \pi/2$ *and* $\ddot{r}_r(t) = 0$ *for all time* $t \geq t_f$ *with some* $t_f < \infty$:

$$\ddot{r} = \ddot{r}_r - K_v\left[(\dot{r} - \dot{r}_r) - 2\beta\frac{\theta}{\cos\theta}\right], \quad (5)$$

where β *is an anti-swing control gain satisfying* $\beta \geq 1.5|\dot{l}|$ *for all time* $t \geq 0$; $\dot{r}_r(t)$ *is a time-varying velocity reference*

of the trolley to be determined later; K_v *is a sufficiently-large positive constant such that the bandwidth of the first-order low-pass filter* (5) *is sufficiently larger than the frequency content of* $\theta/\cos\theta$.

Remark 1: The swing angle of the kinematic model (4) can be controlled by using the trolley acceleration $\ddot{r}$; that is, the swing angle can be suppressed to zero if $\ddot{r}$ is controlled such that $\ddot{r} = \beta\dot{\theta}$, or equivalently $\dot{r} = \beta\theta$, with large β. At the same time, the trolley velocity $\dot{r}$ should track a given time-varying velocity reference $\dot{r}_r$. As a consequence, $\dot{r} = \dot{r}_r + \beta\theta$ should be satisfied in the motion planning. In this study, $\dot{r} = \dot{r}_r + \beta\theta$ is accomplished by using a first-order low-pass filter $(\ddot{r} - \ddot{r}_r) + K_v(\dot{r} - \dot{r}_r) = K_v\beta\theta$, the structure of which is the same as that of equation (5), with a large value of K_v. When K_v (the corner frequency or the bandwidth of the low-pass filter) is much larger than the frequency content of θ, the output $(\dot{r} - \dot{r}_r)$ tracks the input $(\beta\theta)$ with the tracking error decaying exponentially to zero, thus resulting in $(\dot{r} - \dot{r}_r) = \beta\theta$, which is equivalent to $\dot{r} = \dot{r}_r + \beta\theta$. In the theorem, however, $\beta\theta/\cos\theta$ is used instead of $\beta\theta$ to improve the stability as shown in the stability proof.

Remark 2: The proposed anti-swing control (5) is designed not to control an overhead crane but to generate a desired anti-swing trajectory for the overhead crane. The proposed anti-swing control (5) is a model-following anti-swing control; that is, the trolley velocity $\dot{r}$ follows its time-varying velocity reference $\dot{r}_r(t)$ while suppressing the resulting load swing by using $\beta\theta/\cos\theta$. On the other hand, the anti-swing controls proposed in the previous study (Lee 2002, 2004) are regulating anti-swing controls around a constant trolley velocity.

Proof: Suppose that K_v is sufficiently larger than the frequency content of $\theta/\cos\theta$. Then, according to Remark 1, the following approximation is well justified:

$$\dot{r} = \dot{r}_r + 2\beta\frac{\theta}{\cos\theta}, \tag{6}$$

which is differentiated with respect to time to compute $\ddot{r}$:

$$\ddot{r} = \ddot{r}_r + 2\beta\left(\frac{1}{\cos\theta} + \frac{\theta\sin\theta}{\cos^2\theta}\right)\dot{\theta}. \tag{7}$$

Then the kinematic model (4) with $\ddot{r}$ computed in Eq. (7) can be rewritten as

$$l\ddot{\theta} + 2\left(\beta + \dot{l} + \beta\frac{\theta\sin\theta}{\cos\theta}\right)\dot{\theta} + g\sin\theta = -\cos\theta\ddot{r}_r. \tag{8}$$

Now, consider the following Lyapunov function candidate:

$$V = \frac{1}{2}l\dot{\theta}^2 + g(1 - \cos\theta) \geq 0, \tag{9}$$

where $|\theta(0)| < \pi/2$.

Taking the time derivative of V along the trajectories of the kinematic system (8) yields

$$\begin{aligned}\dot{V} &= l\dot{\theta}\ddot{\theta} + \frac{1}{2}\dot{l}\dot{\theta}^2 + g\sin\theta\dot{\theta} \\ &= -\left(2\beta + \frac{3}{2}\dot{l} + 2\beta\frac{\theta\sin\theta}{\cos\theta}\right)\dot{\theta}^2 - \cos\theta\ddot{r}_r\dot{\theta} \\ &= -\beta\left(1 + 2\frac{\theta\sin\theta}{\cos\theta}\right)\dot{\theta}^2 - \left(\beta + \frac{3}{2}\dot{l}\right)\dot{\theta}^2 - \cos\theta\ddot{r}_r\dot{\theta} \\ &\leq -\beta\left(\frac{1}{2} + 2\frac{\theta\sin\theta}{\cos\theta}\right)\dot{\theta}^2 - \frac{\beta}{2}\left(\dot{\theta} + \frac{\cos\theta\ddot{r}_r}{\beta}\right)^2 + \frac{\ddot{r}_r{}^2}{2\beta}\cos^2\theta.\end{aligned} \tag{10}$$

The trolley acceleration reference $\ddot{r}_r$ is designed to be uniformly bounded. Therefore, the $\theta\sin\theta/\cos\theta$ term guarantees $|\theta(t)| < \pi/2$ for all time $t \geq 0$ since $\cos\theta \to 0$ and hence $\dot{V} \to -\infty$ as $|\theta| \to \pi/2$. In addition, equation (10) is reduced to $\dot{V} \leq -\beta\dot{\theta}^2/2 + \cos^2\theta\ddot{r}_r{}^2/(2\beta)$, and hence $\dot{V} \leq 0$ is guaranteed for all $\dot{\theta}$ satisfying $\dot{\theta}^2 \geq \cos^2\theta\ddot{r}_r{}^2/\beta^2$. As a result, $\dot{\theta} \in L_\infty$ follows from the definition of $V(t)$. Then $\dot{r} \in L_\infty$, $\ddot{r} \in L_\infty$, and $\ddot{\theta} \in L_\infty$ result from equations (6), (7), and (8), respectively.

$\ddot{r}_r(t)$ is designed to be uniformly bounded for all time $t \geq 0$ and to be zero for all time $t \geq t_f$, with some $t_f < \infty$. Then, integration of $\cos^2\theta\ddot{r}_r{}^2/(2\beta)$ from zero to infinity is bounded, and hence integration of $\dot{V}$ from zero to infinity yields $\dot{\theta} \in L_2$. Since $\ddot{\theta} \in L_\infty$, as a consequence of Barbalet's Lemma, $\dot{\theta} \to 0$ asymptotically as $t \to \infty$, which guarantees $\ddot{\theta} \to 0$ asymptotically as $t \to \infty$ since $\ddot{\theta} \in L_\infty$. Then, equation (8) guarantees $\theta \to 0$ asymptotically as $t \to \infty$, and thus equation (6) guarantees $\dot{r} \to \dot{r}_r$ asymptotically as $t \to \infty$. Q.E.D.

Remark 3: Optimum damping is critical for a high-performance anti-swing control, especially in the constant-velocity zone and at goal positions. In the constant-velocity zone and at goal positions, $\ddot{r}_r$ and $\dot{l}$ are all zero. Then, with small swing angle, the differential equation (8) can be linearized as $l\ddot{\theta} + 2\beta\dot{\theta} + g\theta = 0$. In this case, the optimum damping β is found to be $\beta = \zeta(gl)^{1/2}$, where ζ denotes the damping ratio of the load swing. The $\theta\sin\theta/\cos\theta$ term increases the damping when the swing angle is not small.

Remark 4: As long as the anti-swing gain β is selected as $\beta \geq 1.5|\dot{l}|$, the proposed anti-swing control (5) guarantees asymptotic stability with $\ddot{r}_r = 0$, regardless of $\dot{l}$,

as shown in equation (10). Therefore, the control law allows any pattern of load hoisting; e.g. hoisting down in the accelerating zone and hoisting up in the decelerating zone. In addition, the load can be hoisted up and/or down in the constant-velocity zone, if necessary. However, no additional load hoisting is normally required in the constant-velocity zone since the load is already hoisted up fully in the accelerating zone.

Remark 5: $|\theta(t)| < \pi/2$ for all time $t \geq 0$ as proven above. In addition, $\dot{\theta} \to 0$ and $\theta \to 0$ asymptotically as $t \to \infty$, with $\ddot{r}_r = 0$ and $\dot{l} = 0$ in the constant velocity zone and at a goal position. Then integration of the kinematic system (8) implies that $\int_0^t \theta \, d\tau$ and hence $\int_0^t \theta / \cos\theta \, d\tau$ are bounded. Integration of the trolley velocity (6) shows that the trolley position r approaches $r_r + 2\beta \int_0^t \theta / \cos\theta \, d\tau$ instead of r_r. This problem will be fixed in the motion planning in the next section.

4. Proposed motion planning

In this section, a new motion-planning method will be proposed for a two-dimensional overhead crane based on the model-following anti-swing control law (5), which requires the design of the trolley velocity reference $\dot{r}_r(t)$ and acceleration reference $\ddot{r}_r(t)$. First, the trolley reference ($\ddot{r}_r$ and $\dot{r}_r$) and load-hoisting trajectory ($\ddot{l}$, $\dot{l}$, and l) will be designed. Then the desired trajectories $\ddot{r}$, $\dot{r}$, r, $\ddot{\theta}$, $\dot{\theta}$, and θ will be generated using the model-following anti-swing control law (5) with the trolley reference and load-hoisting trajectory.

In this study, typical anti-swing crane operation in practice will be taken into account in the trajectory generation; that is, the crane load is hoisted up in the accelerating zone, is moved with zero swing in the constant-velocity zone, and is hoisted down in the decelerating zone.

4.1. *Trajectory references*

As velocity references for the trolley and hoisting motion, smooth velocity profiles will be employed for smooth low-jerk motion. Figure 2 shows the smooth velocity profiles $\dot{r}_r$ used in this study, where $v_{\max}$ denotes the maximum velocity; t, t_a, t_c, and t_d denote the time, accelerating interval, constant-velocity interval, and decelerating interval, respectively. The trajectory reference r_r can be obtained by integrating $\dot{r}_r$.

In the accelerating zone ($0 \leq t \leq t_a$), shown in figure 2, the velocity $\dot{r}_r$ and acceleration $\ddot{r}_r$ are designed as

$$\dot{r}_r(t) = \frac{v_{\max}}{2}\left(1 - \cos\frac{\pi}{t_a}t\right), \tag{11}$$

$$\ddot{r}_r(t) = \frac{\pi v_{\max}}{2t_a}\sin\frac{\pi}{t_a}t. \tag{12}$$

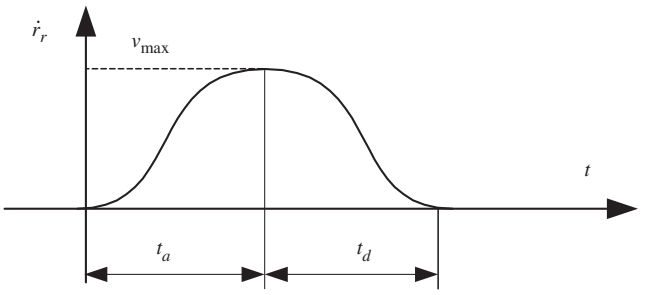

(a) Velocity profile for short travelling

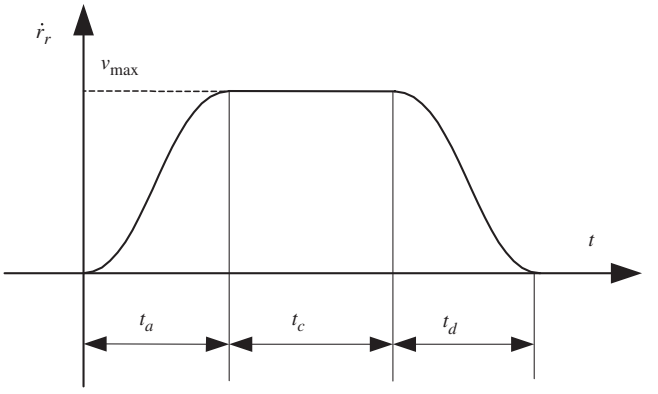

(b) Velocity profile for long travelling

Figure 2. Velocity profiles for trajectory references.

In the decelerating zone, defined with $(t_a + t_c) \leq t \leq (t_a + t_c + t_d)$, the velocity $\dot{r}_r$ and deceleration $\ddot{r}_r$ are designed as

$$\dot{r}_r(t) = \frac{v_{\max}}{2}\left[1 + \cos\frac{\pi}{t_d}(t - t_a - t_c)\right], \tag{13}$$

$$\ddot{r}_r(t) = -\frac{\pi v_{\max}}{2t_d}\sin\frac{\pi}{t_d}(t - t_a - t_c). \tag{14}$$

From equations (12) and (14), the maximum acceleration ($\dot{v}_{a\max}$) and maximum deceleration ($\dot{v}_{d\max}$) of the velocity references are obtained as $\dot{v}_{a\max} = \pi v_{\max}/2t_a$ and $\dot{v}_{d\max} = \pi v_{\max}/2t_d$, respectively. Therefore, for given maximum available velocity and acceleration of the trolley and hoisting systems, the minimum accelerating interval ($t_{a\min}$) and the minimum decelerating interval ($t_{d\min}$) can be computed as

$$t_{a\min} = \frac{\pi}{2}\cdot\frac{v_{\max}}{\dot{v}_{a\max}}, \qquad t_{d\min} = \frac{\pi}{2}\cdot\frac{v_{\max}}{\dot{v}_{d\max}}. \tag{15}$$

4.2. *Motion planning*

As a preliminary step of the motion planning, set a trial travelling distance r_t equal to a given desired travelling distance r_g of the trolley.

Step 1: Compute the accelerating and decelerating intervals based on the period of load swing computed with an appropriate constant rope length (e.g. the average or maximum rope length). The accelerating and decelerating intervals should be equal to or greater than their minimum values computed in equation (15). The total hoisting-up time is set equal to or less than the accelerating interval, and the total hoisting-down time is set equal to or less than the decelerating interval.

Step 2: Generate the hoisting-up and hoisting-down trajectories l, $\dot{l}$, and $\ddot{l}$ in the accelerating and decelerating zones independently of the trolley motion and load swing. The load should be hoisted up to a level higher than any obstacles in the workspace. For given hoisting distance, maximum hoisting velocity, and maximum hoisting acceleration, generate the hoisting trajectories by using one of the velocity profiles shown in figure 2. For this, use a negative value of $v_{\max}$ for the hoisting-up motion and a positive value of $v_{\max}$ for the hoisting-down motion.

Step 3: Determine the trolley velocity reference $\dot{r}_r(t)$. For given maximum available trolley velocity $v_{\max}$, compute the total travelling distance in the accelerating and decelerating zones based on the short-travelling velocity profile shown in figure 2(a). If the total travelling distance is greater than the trial travelling distance r_t, reduce $v_{\max}$ such that the total travelling distance is equal to the trial travelling distance r_t. If the total travelling distance is smaller than or equal to the trial travelling distance r_t, compute the constant-velocity interval (t_c) of the long-travelling velocity profile shown in figure 2(b).

Step 4: Compute the trolley trajectory r, $\dot{r}$, and $\ddot{r}$ and the load-swing trajectory θ, $\dot{\theta}$, and $\ddot{\theta}$ by integrating the kinematic equation (4) and the model-following anti-swing control law (5). For this, use the accelerating and decelerating intervals computed in Step 1, the hoisting trajectory computed in Step 2, and the trolley velocity reference $\dot{r}_r$ determined in Step 3.

Step 5: Compute and minimize the trolley travelling error, the difference between the desired trolley travelling distance r_g and the actual trolley travelling distance r at the end of decelerating zone. If the trolley travelling error $(r_g - r)$ is positive, increase the trial travelling distance r_t based on the trolley travelling error and return to Step 3. If the trolley travelling error $(r_g - r)$ is negative, reduce the trial travelling distance r_t based on the trolley travelling error and return to Step 3. Repeat this process until the trolley travelling error is sufficiently small (i.e., $|r_g - r| < \gamma$ for a sufficiently small threshold γ).

Step 6: Generate the desired trajectories $\ddot{r}$, $\dot{r}$, r, $\ddot{l}$, $\dot{l}$, l, $\ddot{\theta}$, $\dot{\theta}$, and θ in real time for anti-swing trajectory control. For this, repeat Steps 2, 3, and 4 with the accelerating and decelerating intervals computed in Step 1, the maximum trolley velocity $v_{\max}$ reset in Step 3, and the trial trolley travelling distance r_t determined in Step 5.

Remark 6: The proposed method consists of an off-line motion planning and a real-time trajectory generation in series. First, in the off-line motion planning, the accelerating and decelerating intervals are determined and the maximum trolley velocity $v_{\max}$ and trial travelling distance r_t are reset by carrying out Steps 1–5. This off-line motion planning involves iterations, which normally take less than one second with a Pentium III computer. Next, in the real-time trajectory generation, the desired trajectories $\ddot{r}$, $\dot{r}$, r, $\ddot{l}$, $\dot{l}$, l, $\ddot{\theta}$, $\dot{\theta}$, and θ are computed in real time without iterations, by executing Steps 2–4 with the accelerating and decelerating intervals t_a and t_d, the maximum trolley velocity $v_{\max}$, and the trial travelling distance r_t, determined in the off-line motion planning. Therefore, the proposed method has no problems in generating real-time trajectories.

Remark 7: In the open-loop motion planning proposed by Mita and Kanai (1979), the accelerating and decelerating intervals t_a and t_d are fixed for a given hoisting rope length. However, in the proposed trajectory generation, based on the model-following anti-swing control law (5), t_a and t_d can be arbitrarily set as long as they are greater than their minimum values given in equation (15). In addition, the model-following anti-swing control law allows any pattern of $\dot{r}_r$ as long as $\ddot{r}_r$, $\dot{r}_r$, and r_r are all uniformly bounded. Therefore, the proposed method is not limited to the triangular and trapezoidal velocity profiles used in Mita and Kanai's method.

Remark 8: The previous motion-planning method (Lee 2002, 2004) applies a minimum-time open-loop control and a regulating anti-swing control in series, in each of the accelerating and decelerating zones. As a result, load swing is not controlled while the minimum-time control is applied; therefore, the performance of trajectory generation deteriorates when the maximum available trolley acceleration is not sufficient for a minimum-time control. On the other hand, the proposed motion-planning method applies the model-following anti-swing control law (5) throughout the entire motion planning. As a result, the proposed method is not influenced by the accelerating and decelerating intervals and hence not influenced by the maximum available trolley acceleration.

5. Motion planning for three-dimensional overhead cranes

In this study, a practical motion-planning method is proposed for a three-dimensional overhead crane,

without solving its complicated load-swing dynamics. For this, the motion planning method proposed for a two-dimensional overhead crane is extended for its three-dimensional counterpart, based on their geometric relationships shown in figure 3. This approach is well justified since the motion planning is not a dynamic problem, but a kinematic problem.

Remark 9: The proposed motion planning described in the previous section can be extended for a three-dimensional overhead crane based on its own load-swing dynamics. A major problem in this case is that the load-swing dynamics of a three-dimensional overhead crane (Moustafa and Ebeid 1988, Lee 1998) is much more complicated than that of a two-dimensional overhead crane. As a result, the design of a model-following anti-swing control corresponding to equation (5) will be substantially complicated and difficult.

In this study, it is assumed that the overhead cranes are controlled over convex workspaces (e.g. the square or rectangular workspaces normally used in industry). It is also assumed that the load is hoisted up in the accelerating zone and hoisted down in the decelerating zone to avoid all possible obstacles in the workspace. Then the trolley can be controlled along the straight line from a starting position $(x_s, y_s, 0)$ to a goal position $(x_g, y_g, 0)$ for a minimum-time control. If the workspace is concave for any reason, the trolley trajectories can be divided into a series of straight-line trajectories, each of which can be generated using the proposed method to be described below.

In figure 3, XYZ is the inertial reference coordinate system. RZ_r is the two-dimensional trolley coordinate system used in figure 1. RZ_r is defined based on the starting position $(x_s, y_s, 0)$ and goal position $(x_g, y_g, 0)$ of the trolley in the XYZ coordinate system. The origin of RZ_r, $(0, 0)$, is located at the starting position $(x_g, y_g, 0)$ and the trolley is located at $(r, 0)$ in the RZ_r frame. $X_T Y_T Z_T$ is a three-dimensional trolley coordinate system moving with the trolley (Lee 1998), whose origin is attached to the trolley located at $(x, y, 0)$ in the XYZ coordinate system. The Y_T axis is defined on and along the girder which is not shown in the figure. The trolley moves on the girder in the Y_T direction and the girder (Y_T axis) moves in the X_T direction. θ is the swing angle of the load in space (in the RZ_r plane) and has two components θ_x and θ_y in the $X_T Y_T Z_T$ coordinate system; θ_x is the swing angle projected onto the $X_T Z_T$ plane and θ_y is the swing angle measured from the $X_T Z_T$ plane. ϕ is the swirling angle of the load around the Z_T axis.

For the given starting position $(x_s, y_s, 0)$ and goal position $(x_g, y_g, 0)$ of the trolley, the desired travelling distance r_g is computed, where the goal position $(x_g, y_g, 0)$ in the XYZ coordinate system corresponds to a point $(r_g, 0)$ in the RZ_r coordinate system, as shown in figure 3. Then the desired trajectories ($\ddot{r}$, $\dot{r}$, r, $\ddot{l}$, $\dot{l}$, l, $\ddot{\theta}$, $\dot{\theta}$, and θ) in the RZ_r plane are computed by using the proposed motion planning for a two-dimensional crane described in the previous section. Finally, the trajectories for the corresponding three-dimensional crane are computed from those for the two-dimensional

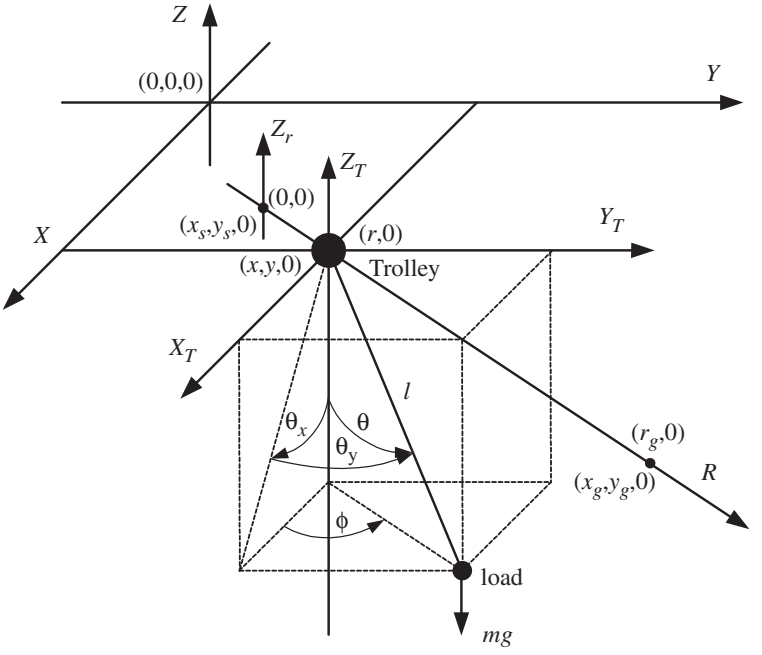

Figure 3. Two- and three-dimensional models of an overhead crane.

crane, based on their geometric relationships shown in figure 3.

First, the constant swirling angle ϕ is computed as

$$\phi = \tan^{-1}\left(\frac{y_g - y_s}{x_g - x_s}\right), \tag{16}$$

which can be used as the desired reference trajectory of the swirling angle ϕ when the spherical coordinate system is used in the dynamic model (Moustafa and Ebeid 1988).

Second, the desired trajectories of the two-dimensional trolley motion in the XYZ coordinate system can be computed as

$$\begin{aligned} x &= \cos\phi r + x_s, \quad \dot{x} = \cos\phi \dot{r}, \quad \ddot{x} = \cos\phi \ddot{r}, \\ y &= \sin\phi r + y_s, \quad \dot{y} = \sin\phi \dot{r}, \quad \ddot{y} = \sin\phi \ddot{r}. \end{aligned} \tag{17}$$

Finally, the desired trajectories of the swing angles θ_x and θ_y can be computed based on the geometry shown in figure 3:

$$\begin{aligned} \theta_x &= \tan^{-1}(\tan\theta\cos\phi), \\ \theta_y &= \sin^{-1}(\sin\theta\sin\phi). \end{aligned} \tag{18}$$

Then $\dot{\theta}_x$ and $\ddot{\theta}_x$ can be readily computed by differentiating θ_x with respect to time, and $\dot{\theta}_y$ and $\ddot{\theta}_y$ can also be computed by differentiating θ_y with respect to time. Note that $\ddot{\theta}$, $\dot{\theta}$, and θ are computed in the trajectory generation of the corresponding two-dimensional overhead crane.

6. Evaluation of the proposed motion planning

The effectiveness of the proposed motion planning has been validated by generating high-performance anti-swing trajectories for a two-dimensional overhead crane defined in the RZ_r coordinates in figure 3. High-performance anti-swing trajectories for the corresponding three-dimensional overhead crane can be readily computed by using equations (16)–(18).

Based on Theorem 1 and Remark 3, the following parameters were selected for optimal anti-swing control in the trajectory generation: $K_v = 1000$ and $\beta = \zeta(gr_l)^{1/2}$ with $\zeta = 0.8$, where r_l was selected as the desired average rope length for the accelerating and constant-velocity zones and as the desired maximum rope length for the decelerating zone. The maximum trolley velocity was limited by setting $v_{\max}$. In this motion planning, $v_{\max}$ is 1.5 m/s, and the maximum trolley acceleration was set to 1 m/s^2.

As described in Remark 7, the proposed motion planning allows flexible accelerating and decelerating intervals (t_a and t_d); that is, they can be arbitrarily set as long as they are equal to or greater than their minimum values given in equation (15). In this motion planning, the accelerating interval (t_a) was set to 60% of one swing period computed with the maximum rope length in this zone. The decelerating interval (t_d) was set to 60% of one swing period computed with the average rope length in this zone.

The trapezoidal rule was used for the integration of the kinematic model (4) and the model-following anti-swing control law (5). The integration interval was chosen to be 1 ms. When a large sampling period is used in real-time anti-swing control, multiple integrations can be performed in one sampling period with the integration interval set equal to a fraction of one sampling period, or the fourth-order Runge-Kutta formula (Press *et al*. 1986) can be used with the integration interval set equal to the sampling period.

As described in Remark 6, the off-line motion planning involves iterations, but the trial travelling distance r_t converges substantially fast to its desired value; e.g. without an iteration for a constant rope length and with less than three iterations for high-speed long-distance load hoisting. The anti-swing trajectories are generated in real-time without iterations after the off-line motion planning is completed.

Figures 4, 5 and 6 show the results of trajectory generation for short, medium, and long trolley travelling, respectively. Figure 7 shows the results of trajectory generation for long trolley travelling with long accelerating and decelerating intervals. As in practice, load hoisting was not considered for the short trolley travelling as seen in figure 4. However, for the medium and long travelling, the load was hoisted up in the accelerating zone and hoisted down in the decelerating zone as shown in figures 5, 6 and 7 in order to avoid various obstacles in the workspace.

The load swing is zero in the constant-velocity zone and at the goal positions as shown in figures 5, 6 and 7. The position errors of the trolley travelling, load hosting, and load swing are also all zero in the constant-velocity zone and at the goal positions. This shows that the anti-swing control law (5) guarantees asymptotic stability in the constant-velocity zone and at the goal positions. In addition, the swing-angle trajectories include neither an overshoot nor an undershoot in the constant-velocity zone and at the goal positions, which shows that the proposed control guarantees optimum damping for the load swing in both the accelerating and decelerating zones.

The hoisting speed is very high and the hoisting distance is also very large for the medium and long trolley travelling, as shown in figures 5 and 6. The rope length

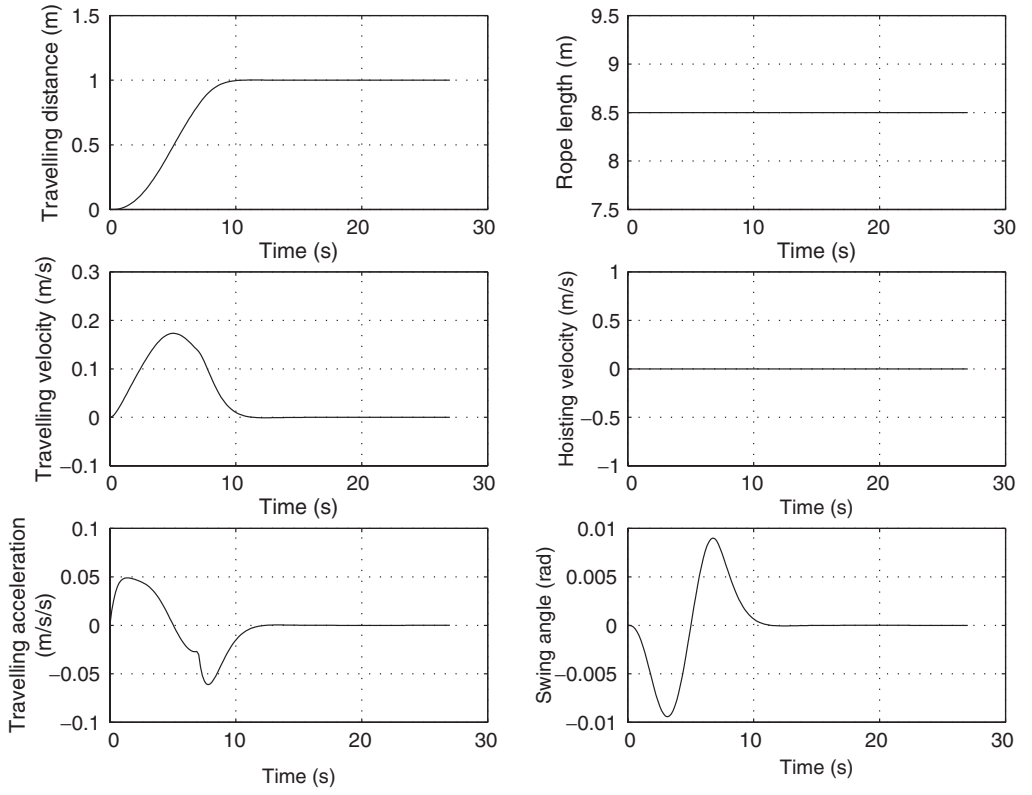

Figure 4. Trajectory generation for a short travelling distance (1 m).

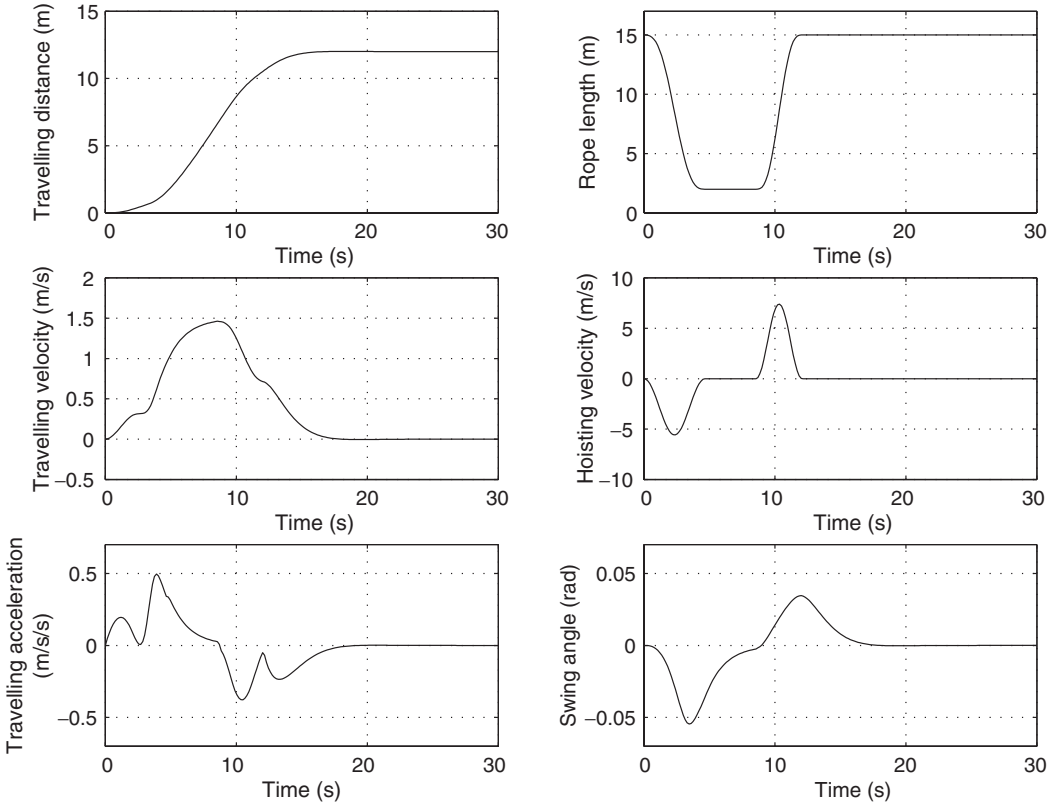

Figure 5. Trajectory generation for a medium travelling distance (12 m).

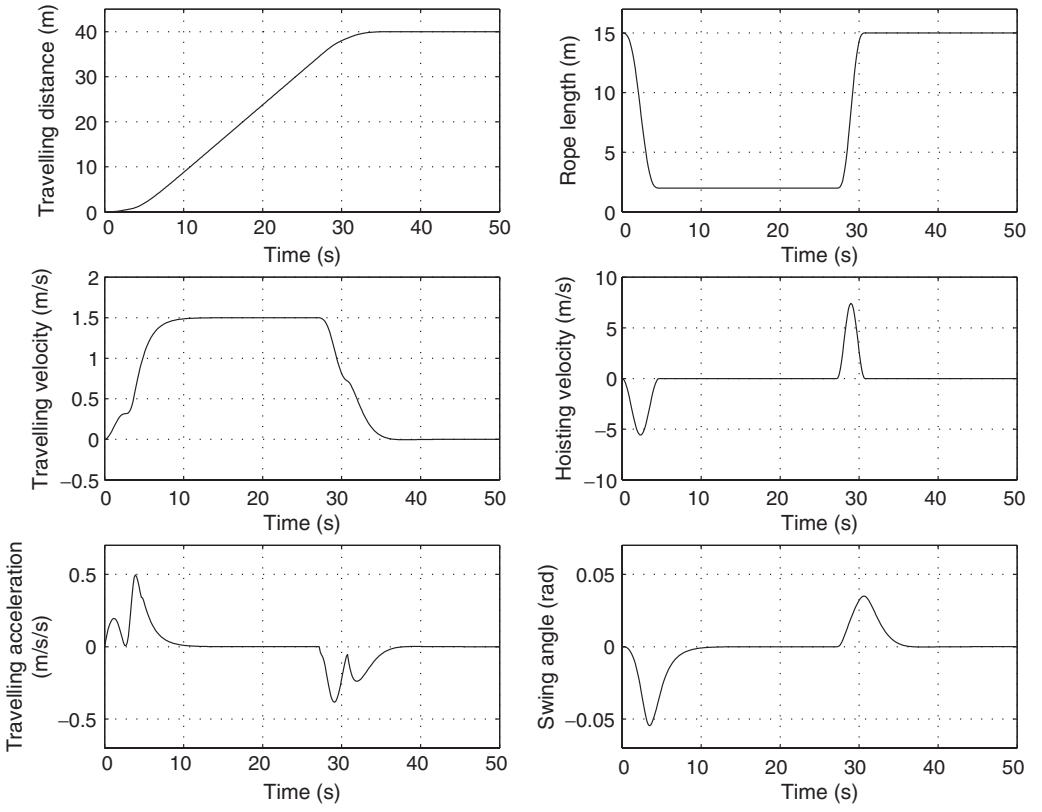

Figure 6. Trajectory generation for a long travelling distance (40 m).

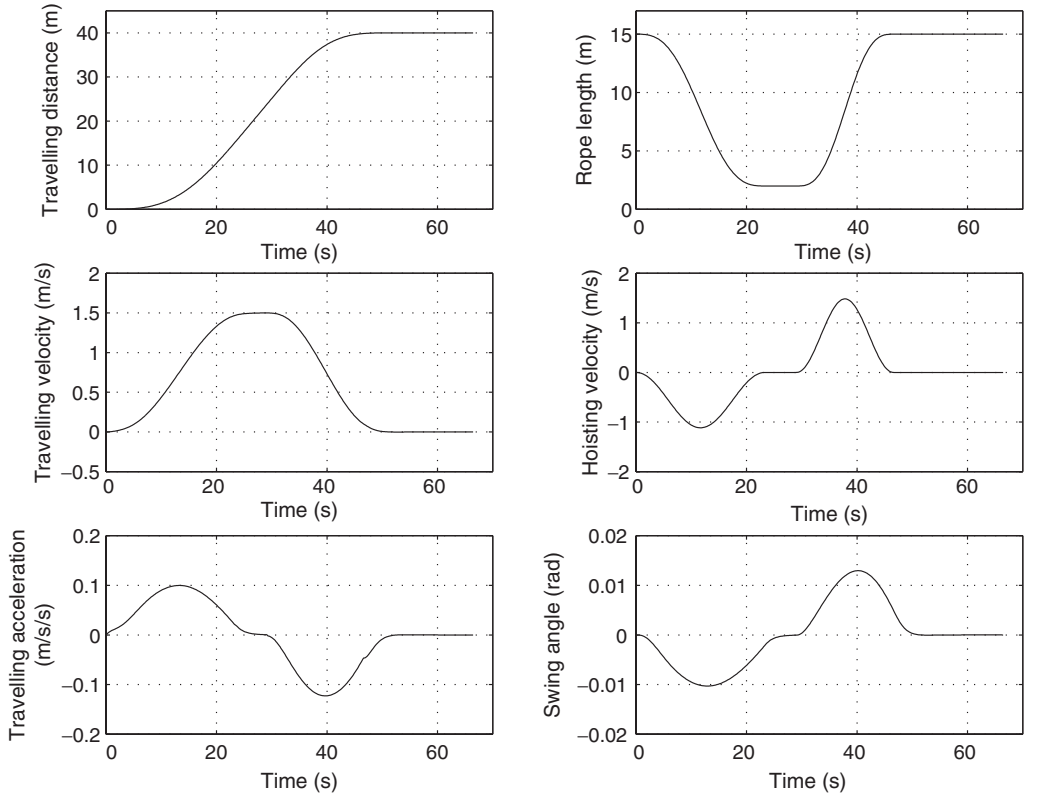

Figure 7. Trajectory generation for a long travelling distance (40 m) with long accelerating and decelerating intervals.

was reduced from 15 m to 2 m in the accelerating zone and was increased from 2 m back to 15 m in the decelerating zone in order to simulate worst-case crane operations in practice. The hoisting ratio (the ratio of the maximum to minimum rope length) is also very high. However, the load-swing angle is kept relatively small, which is critically important from the safety point of view. This trajectory generation covers all possible worst-case crane operations in practice.

The hoisting-up motion ($\dot{l} < 0$) reduces the damping and the hoisting-down motion ($\dot{l} > 0$) increases the damping, as can be seen in equation (8). Therefore, the swing angle in the accelerating zone is greater than that in the decelerating zone, as shown in figures 5 and 6. According to Remark 7, the accelerating interval can be readily increased to reduce the swing angle in the accelerating zone. The decelerating interval can be also decreased if required; then the swing angle will be increased in the decelerating zone.

The rope length for the short travelling is 8.5 m as shown in figure 4. Then one swing period is computed as 5.84 ($2\pi/\sqrt{g/8.5}$) seconds, which is the accelerating (and also decelerating) interval of a minimum-time anti-swing trajectory with the constant rope length (Mita and Kanai 1979). However, each of the accelerating and decelerating intervals shown in figure 4 is about 5.5 seconds, less than 5.84 seconds, which implies that the proposed motion-planning method generates a near-minimum-time anti-swing trajectory, at least with a constant rope length. However, as the hoisting speed and ratio increase, the accelerating and decelerating intervals also increase, as shown in figures 5 and 6.

The performance of the trajectory generation is minimally affected by the accelerating and decelerating intervals, as shown in figures 6 and 7. The accelerating and decelerating intervals in figure 7 are five times as large as those in figure 6. When the intervals are short as seen in figure 6, the trolley acceleration is high and includes a notch to suppress the large load swing caused by the high trolley acceleration. In summary, figures 6 and 7 show that the performance of the proposed motion planning is not affected by the accelerating and decelerating intervals and hence not affected by the maximum available trolley acceleration. As a result, the proposed motion planning can be applied to any existing overhead cranes without increasing their actuator torque capacity.

Finally, it should be emphasized that the proposed motion planning has no application problems since the kinematic model (4) is free from parametric uncertainties, disturbances, and signal measurements in the process of motion planning. In addition, the proposed method is practical for real-time application since the off-line computation takes less than one second with a Pentium III computer, and hence can always be completed before the start of real-time trajectory generation.

7. Conclusion

In this paper, a systematic motion-planning method has been proposed for a high-performance anti-swing control, allowing high-speed load hoisting, for three-dimensional overhead cranes. The proposed method is based on the load-swing dynamics of a two-dimensional overhead crane and thus avoids solving the complicated load-swing dynamics of a three-dimensional overhead crane.

The stability of the model-following anti-swing control law has been proven using the Lyapunov stability theorem and has also been shown by generating anti-swing trajectories. In addition, the damping of the anti-swing control law can be set to be optimal. Furthermore, the proposed motion-planning scheme maintains small swing angle for the safe crane operation in spite of high hoisting speed and ratio with high trolley acceleration.

The proposed motion-planning method generates a typical anti-swing trajectory in practice for both two- and three-dimensional overhead cranes, which is free from the usual mathematical constraints in anti-swing control such as small load swing, slow hoisting speed, and small hoisting distance. In addition, the proposed motion planning has no problems for real-time application. Moreover, the performance of the proposed motion planning is not affected by the maximum available trolley acceleration and hence can be applied to any existing overhead cranes without increasing their actuator torque capacity.

In conclusion, the proposed approach can be readily adopted for the generation of high-efficiency anti-swing desired trajectories for both two- and three-dimensional overhead cranes in industry. As a future research, a high-performance anti-swing trajectory control scheme, to be used along with this proposed motion planning, will be developed for two- and three-dimensional overhead cranes in order to actually control their motion in the presence of parametric uncertainties and disturbances.

References

S.-K. Cho and H.-H. Lee, "A fuzzy logic anti-swing controller for three-dimensional overhead crane", *ISA Trans*., 41, pp. 235–243, 2002.

J. Collado, R. Lozano and I. Fantoni, "Control of convey-crane based on passivity", in *Proceedings of American Control Conference*, Chicago, June, 2000, pp. 1260–1264.

B. d'Andrea-Novel and F. Boustany, "Adaptive control of a class of mechanical systems using liniarization and lyapunov methods. A comparative study on the overhead crane example", in *Proceeding of the 30th IEEE Conference on Decision and Control*, Brighton, England, December, 1991, pp. 120–125.

Y. Fang, W. Dixon, D. Dawson and E. Zergeroglu, "Nonlinear coupling control laws for a 3-DOF overhead crane system",

in *Proceedings of the 40th IEEE Conference on Decision and Control*, Orlando, Florida, 2001, pp. 3766–3771.

Y. Fang, W. Dixon, D. Dawson and E. Zergeroglu, "Nonlinear coupling control laws for an underactuated overhead crane system", *IEEE/ASME Trans. on Mechatronics*, 8, pp. 418–423, 2003.

B. Kiss, J. Levine and P. Mullhaupt, "A simple output feedback PD controller for nonlinear cranes", in *Proceedings of the 39th IEEE Conference on Decision and Control*, Sydney, Australia, 2000, pp. 5097–5101.

H.-H. Lee, "Modeling and control of a three-dimensional overhead crane", *ASME Trans., J. of Dynamic Systems, Measurement and Control*, 120, pp. 471–476, 1998.

H.-H. Lee, "A path-planning strategy for overhead cranes with high hoisting speed", in *Proceeding of IMECE 2002*, New Orleans, Paper No.: IMECE2002-DSC-33127, 2002.

H.-H. Lee, "A new approach for the anti-swing control of overhead cranes with high-speed load hoisting", *International Journal of Control*, 76, pp. 1493–1499, 2003.

H.-H. Lee, "A new motion-planning scheme for overhead cranes with high-speed hoisting", *ASME Trans., J. of Dynamic Systems, Measurement and Control*, 126, pp. 359–364, 2004.

H.-H. Lee, D. Segura and Y. Liang, "A new trajectory-generation scheme for overhead cranes with high-speed load hoisting", in *Proceeding of IMECE 2004*, Anaheim, California, Paper number: IMECE2004-59087, 2004.

K.A.F. Moustafa and A.M. Ebeid, "Nonlinear modeling and control of overhead crane load sway", *ASME Trans., J. of Dynamic Systems, Measurement and Control*, 110, pp. 266–271, 1988.

T. Mita and T. Kanai, "Optimal control of the crane system using the maximum speed of the trolley (in Japanese with English abstract)", *Trans. Soc. Instrument. Control Eng. (Japan)*, 15, pp. 833–838, 1979.

W. Press, B. Flannery, S. Teukolsky and W. Vetterling, *Numerical Recipes: The Art of Scientific Computing*, New York: Cambridge University Press, 1986.

W. Singhose, L. Porter, M. Kenison and E. Kriikku, "Effects of hoisting on the input shaping control of gantry cranes", *Control Engineering Practice*, 8, pp. 1159–1165, 2000.

K. Yoshida, "Nonlinear controller design for a crane system with state constraints", in *Proceedings of American Control Conference*, Pennsylvania, 1998, pp. 1277–1283.

J. Yu, F.L. Lewis and T. Huang, "Nonlinear feedback control of a gantry crane", in *Proceedings of American Control Conference*, Seattle, 1995, pp. 4310–4315.